

## 셸 앤 플레이트 열교환기에서의 R-410A 증발열전달에 관한 실험적 연구

박재홍† · 김인관\* · 김영수\*\*

(원고접수일 : 2004년 10월 11일, 심사완료일 : 2004년 12월 21일)

### Experimental Study on R-410A Evaporation Heat Transfer Characteristics in Shell and Plate Heat Exchanger

Jae-Hong Park† · In-Kwan Kim\* · Young-Soo Kim\*\*

**Abstract :** The evaporation heat transfer experiments are conducted with the shell and plate heat exchanger (S&PHE) without oil in the refrigerant loop using R-410A. An experimental refrigerant loop has been established to measure the evaporation heat transfer coefficient  $h_r$  of R-410A in a vertical S&PHE. Two vertical counter flow channels were formed in the S&PHE by three plates having a corrugated trapezoid shape of a 45° chevron angle. Up flow of the boiling R-410A in one channel receives heat from the hot down flow of water in the other channel. The effects of the refrigerant mass flux, average heat flux, refrigerant saturation temperature and vapor quality are explored in detail. Similar to the case of a plate heat exchanger, even at a very low Reynolds number, the flow in the S&PHE remains turbulent. The present data shows that the evaporation heat transfer coefficients of R-410A increased with the vapor quality. The results indicate a rise in the refrigerant mass flux caused an increase in the  $h_r$ . Raising the imposed wall heat flux is found to slightly improve  $h_r$ , while  $h_r$  is found to be lower at a higher refrigerant saturation temperature. Based on the present data, empirical correlation of the evaporation heat transfer coefficient is proposed.

**Key words :** Shell and plate heat exchanger, R-410A, Evaporation, Heat transfer coefficient

#### Nomenclature

$A$ : heat transfer area of the plate [m <sup>2</sup> ]	$Bo$ : Boiling number
$b$ : channel spacing [m]	$c_p$ : specific heat [J/kgK]
	$D_h$ : hydraulic diameter [m]
	$G$ : mass flux [kg/m <sup>2</sup> s]

† 책임저자(부경대학교), E-mail : parksonforever@hanmail.net, T : 051)620-1503

\* 부경대학교 RRC

\*\* 부경대학교 기계공학부

$h$  : heat transfer coefficient [W/m<sup>2</sup>K]  
 $i_{fg}$  : enthalpy of vaporization [J/kg]  
 $\dot{m}$  : mass flow rate [kg/s]  
 Nu : Nusselt number  
 Pr : Prandtl number  
 $Q$  : heat transfer rate [W]  
 $q_w''$  : average imposed wall heat flux [W/m<sup>2</sup>]  
 Re : Reynolds number  
 $U$  : overall heat transfer coefficient [W/m<sup>2</sup>K]  
 $u$  : velocity [m/s]  
 $w$  : channel width of the plate [m]  
 $x$  : vapor quality

### Greek symbols

$\Delta T$  : temperature difference [°C]  
 $\Delta x$  : quality change  
 $\rho$  : density [kg/m<sup>3</sup>]

### Subscripts

$eq$  : equivalent  
 $h$  : hot  
 $i, o$  : inlet and outlet  
 $l$  : liquid  
 $lat, sens$  : latent and sensible heats  
 $p$  : pre-heater  
 $r$  : refrigerant  
 $sat$  : saturation  
 $t$  : test section  
 $v$  : gas  
 $w$  : water

## 1. Introduction

Many refrigeration and air conditioning systems have long used R-22 as the working fluid. Recently, because of the

phase out of CFCs and HCFCs outlined by the Montreal Protocol, R-22 will be phased out early this century. As a result, the search for a replacement for R-22 has been intensified in recent years. R-410A, a mixture of 50 wt% R-32 and 50 wt% R-125 that exhibits azeotropic behavior has been considered one of the primary replacements for R-22 in refrigeration and air conditioning systems. Moreover, in view of space saving and tightening energy-efficiency standards imposed by the federal government, the design of more compact heat exchangers is relatively important. Also, to meet the demand for saving energy and resources today, manufacturers are trying to enhance efficiency and reduce the size and weight of heat exchangers. When compared with the well established shell and tube heat exchangers, the plate heat exchanger (PHE) shows a lot of advantages, such as high NTU values, compactness, low cost, multi duties and reduced fouling, etc. PHEs have been widely used in food processing, chemical reaction processes, and other industrial applications for many years. The advantage of using PHE was clearly indicated in the studies from Kerner et al.<sup>(1)</sup> and Williams<sup>(2)</sup>. Particularly, in the last 20 years PHEs have been introduced to air conditioning and refrigeration systems as evaporators or condensers for their high efficiency and compactness.

The shell and plate heat exchanger (S&PHE) is different from the conventional PHE. The plates that have an oblique pattern are circular in shape and stacked together in crisscross pattern.

which are enclosed in a cylindrical shell. The operating temperature up to 350°C, and pressure up to 10 MPa can be achieved. Although the S&PHE looks different from the conventional rectangular PHE, the underlying flow channel configuration is the same as the conventional PHE. The S&PHE is being introduced to refrigeration and air conditioning systems as evaporators or condensers for its high efficiency and compactness. However, there are a little data available for the design of S&PHE to be used as evaporators and condensers.<sup>(3)-(4)</sup>

In this study, the characteristics of the evaporation heat transfer for R-410A flowing in the S&PHE were experimentally explored to set up data base for the design of the S&PHE.

## 2. Experimental apparatus and method

The experimental system and heat transfer plate used to investigate the evaporation heat transfer characteristics of R-410A are shown in Figs. 1 and 2, respectively. The detailed configurations of the S&PHE are given in Table 1. The experimental system consists of a test section, a refrigerant loop, a water loop and a data acquisition unit.

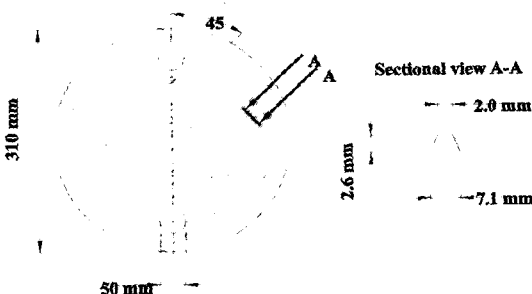


Fig. 2 Schematic diagram of heat transfer plate

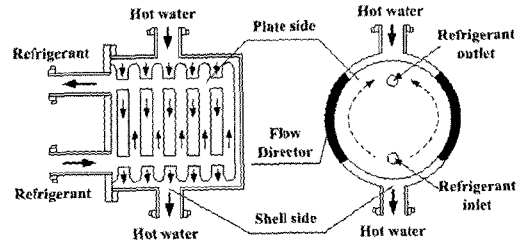


Fig. 3 Details of flow pattern in S&PHE

### 2.1 Test section

Fig. 3 shows the flow direction in the S&PHE. The upflow of R-410A boils by receiving heat from downflow of hot water. Refrigerant R-410A is circulated in the refrigerant loop. In order to obtain different test conditions of R-410A including the vapor quality, saturation temperature (pressure) and heat flux, the temperatures and flow rate of the working fluid in the water loop are controlled.

### 2.2 Refrigerant loop

The refrigerant loop contains a refrigerant pump, a refrigerant flow meter, a pre-heater, a test section (S&PHE), a sub-cooler, a receiver, strainer, a dryer/filter and three sight glasses. The refrigerant pump is a magnetic pump of TUTHILL driven by a DC motor that is, in turn, controlled by a variable DC output motor controller. The variation of the liquid R-410A flow rate is controlled by a rotational DC motor through the change of the DC current. The refrigerant flow rate can also be adjusted by opening the bypass valve. The refrigerant flow rate is measured by a mass flow meter (Oval) installed between the pump and the receiver with

an accuracy of  $\pm 0.2\%$ . The pre-heater is used to evaporate the refrigerant to a specified vapor quality at the test section inlet by transferring heat from heater to R-410A. Note that the amount of heat transfer from pre-heater to refrigerant is calculated from the power meter (YOKOGAWA) connected pre-heater source. The dryer/filter intends to filter the solid particles that possibly present in the loop. Meanwhile, a sub-cooler is used to condense the refrigerant vapor from the test section by a cold water to avoid cavitations at the pump inlet. The pressure of the refrigerant loop can be controlled by varying the temperature and flow rate of cooling water in sub-cooler. After condensed, the subcooled liquid refrigerant flows back to the receiver.

### 2.3 Water loop for test section

The water loop in the system designed for circulating hot water through the test section contains a 200 liter constant temperature water bath with a 5 kW heater and an air cooled refrigeration unit of 1 RT cooling capacity intending to accurately control the water temperature. The hot water is driven by a 0.37 kW water pump with an inverter to the S&PHE with a specified water flow rate. The accuracy of measuring the water flow rate by mass flow meter is  $\pm 0.2\%$ .

### 2.4 Water loop for sub-cooler

The water loop designed for the condensing the R-410A vapor contains 200 liter constant temperature bath with water both with a 5 kW heater and an air

cooled refrigeration unit of 5 RT cooling capacity intending to accurately control the water temperature. Then, a 0.37 kW water pump with an inverter is also used to drive the cool water at a specified water flow rate to the sub-cooler. The supersonic flow meter to measure water flow meter has an accuracy of  $\pm 1\%$ .

### 2.5 Data acquisition

The data acquisition unit includes 20 channels NetDAQ recorder of FLUKE combined with a personal computer. The recorder is used to record the temperature and voltage data. The water flow meter and pressure transducer and differential pressure transducer need a power supply as a driver to output and voltage of 0~10 V. The NetDAQ recorder allows the measured data to transmit to personal computer to be analyzed immediately.

### 2.6 Experimental procedures

In each test the system pressure is maintained at a specified level by adjusting the water loop temperature and its flow rate. The vapor quality of R-410A at the test section inlet can be kept at the desired value by the pre-heater. Finally, the heat transfer rate between the counter flow channels in the test section can be varied by changing the temperature and flow rate in the water loop for the test section. Any change of the system variables will lead to fluctuations in the temperature and pressure of the flow. It takes about 60 min to reach statistically steady state at

which variations of the time-average inlet and outlet temperatures are less than 0.1 °C and the variations of the pressure and heat flux are within 1% and 5%, respectively. Then the data acquisition unit is initiated to scan all the data channels for 60 times in 5 minutes. The mean values of the data for each channel are obtained to calculate the heat transfer coefficient.

### 3. Data reduction

From the definition of the hydraulic diameter, Shah and Wanniarachchi<sup>(5)</sup> suggested to use two times of the channel spacing as the hydraulic diameter for plate heat exchangers when the channel width is much larger than the channel spacing. So we follow this suggestion.

$$D_h \cong 2b = 0.0052 \text{ m} \quad w \gg b \quad (1)$$

The procedures to calculate heat transfer coefficient of the refrigerant flow are described in the following. The total heat transfer rate between the counter flows in the test section is calculated from the hot water side

$$Q_w = \dot{m}_{w,h} c_{p,w} (T_{w,h,i} - T_{w,h,o}) \quad (2)$$

Then, the refrigerant vapor quality entering the test section is evaluated from the energy balance for the pre-heater. The heat transfer to the refrigerant in the pre-heater is the summation of the sensible heat transfer (for the temperature rise of the refrigerant to the saturated value) and latent heat transfer (for the evaporation

of the refrigerant).

$$Q_p = Q_{sens} + Q_{lat} \quad (3)$$

where

$$Q_{sens} = \dot{m}_r c_{p,r} (T_{r,sat} - T_{r,p,i}) \quad (4)$$

$$Q_{lat} = \dot{m}_r i_{fg} x_{p,o} \quad (5)$$

The above equations can be combined to evaluate the refrigerant quality at the exit of pre-heater that is considered to be the same as the vapor quality of the refrigerant entering the test section. Specifically,

$$x_i = x_{p,o} = \frac{1}{i_{fg}} \left( \frac{Q_p}{\dot{m}_r} - c_{p,r} (T_{r,sat} - T_{r,p,i}) \right) \quad (6)$$

The change in the refrigerant vapor quality in the test section is then deduced from the heat transfer to the refrigerant in the test section,

$$\Delta x = \frac{Q_w}{\dot{m}_r \cdot i_{fg}} \quad (7)$$

The average quality in the test section is given as

$$x_m = x_i + \frac{\Delta x}{2} \quad (8)$$

The overall heat transfer coefficient  $U$  between the two counter channel flows can be expressed as

$$U = \frac{Q_w}{A \cdot \Delta T_{LMTD}} \quad (9)$$

The log mean temperature difference (LMTD) is again determined from the inlet and outlet temperatures in the two channels,

$$\Delta T_{LMTD} = \frac{(\Delta T_1 - \Delta T_2)}{\ln(\Delta T_1 / \Delta T_2)} \quad (10)$$

where

$$\Delta T_1 = T_{w,h,i} - T_{r,o} \quad (11)$$

$$\Delta T_2 = T_{w,h,o} - T_{r,i} \quad (12)$$

with  $T_{r,i}$  and  $T_{r,o}$  being the saturation temperature R-410A corresponding respectively to the inlet and outlet pressures in the refrigerant flow in the S&PHE. In view of the same heat transfer area in the refrigerant and water sides, the relation between the overall heat transfer coefficient and the convective heat transfer coefficient on both sides can be expressed as

$$\frac{1}{h_r} = \frac{1}{U} - \frac{1}{h_{w,h}} - R_{wall} \cdot A \quad (13)$$

where the Modified Wilson method<sup>(6)</sup> is applied to calculate  $h_{w,h}$ . In this method, shell side heat transfer correlation is assumed to be that of Sieder-Tate<sup>(7)</sup> type and exponent of the Reynolds number and proportional constant are determined from the experimental data. Experiments are conducted varying the shell side flow rate with the plate side flow rate and the temperature fixed. This method is known to have advantage over the original Wilson plot<sup>(8)</sup> that smaller numbers of test runs are needed. One should be cautious to make both sides of the flow turbulent.

## 4. Results and discussion

### 4.1 Single-phase heat transfer

From the initial single-phase water to water heat transfer test for the S&PHE.

The single heat transfer coefficient in the shell side was correlated by the least square method as

$$N_s = 0.028 Re^{0.92} Pr^{1/3} \text{ for } 800 < Re < 5000 \quad (14)$$

The energy balance between the hot and cold side of water was within  $\pm 5\%$  for all runs. To estimate the uncertainty of single-phase heat transfer coefficient, an uncertainty analysis proposed by Kline and McClintock<sup>(9)</sup> was carried out. The uncertainty of single-phase heat transfer coefficient was within about  $\pm 10\%$ .

### 4.2 Two-phase heat transfer

In the present investigation of the R-410A evaporation in the S&PHE, the R-410A mass flux was varied from 45 to 65 kg/m<sup>2</sup>s, average heat flux from 2.0 to 6.0 kW/m<sup>2</sup> and saturation temperature from 15 to 20°C. The measured heat transfer coefficients are to be presented in terms of their variations with their average vapor quality in the test section. Since the S&PHE is small and has only three plates, the vapor quality change in the test section is small,  $\Delta x < 0.06$ .

Fig. 4 shows the effect of the refrigerant mass flux on the measured R-410A evaporation heat transfer coefficient at saturation temperature of 20°C and an average imposed heat flux of 6.0 kW/m<sup>2</sup> for the mass flux ranging from 45 to 65 kg/m<sup>2</sup>s and the mean vapor quality was varied from 0.1 to 0.75. The results show that the evaporation heat transfer coefficients rise with the increasing of mass flux and for the higher mass flux the heat transfer coefficient rises more quickly than that for the lower mass flux. This is attributed to

the fact that at 20°C the liquid density of R-410A is about 18 times of the corresponding vapor quality. Thus, a great increase in the vapor volume during the evaporation process causes the vapor flow to move in a high speed, which in turn breaks the adjacent liquid film into a large number of tiny liquid droplets in the channel. This highly turbulent mist flow results in a substantial rise in the heat transfer coefficient. The high speed turbulent mist flow continuously wets the heat transfer wall and significantly reduces the resistance of heat transfer from the channel wall to the flow. At a higher mass flux the mist flow is at a higher velocity and the heat transfer is better. It is of interest to note that at  $G=65\text{kg/m}^2\text{s}$  an increase in the vapor quality causes an increase in the heat transfer but for other cases the evaporation heat transfer deteriorates at increasing vapor quality. At  $G=55\text{ kg/m}^2\text{s}$  the fall off in the heat transfer coefficient after the peak ( $x_m=0.5$ ) was observed to be caused by partial dryout. Especially, at the lowest mass flux ( $G=45\text{kg/m}^2\text{s}$ ) the heat transfer coefficient is seen to decrease monotonically with increasing vapor quality.

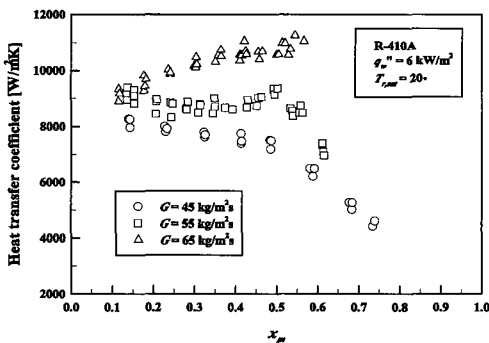


Fig. 4 Variation of evaporation heat transfer coefficient with mean vapor quality for various mass fluxes at  $q_w'' = 6\text{ kW/m}^2$  and  $T_{r,sat} = 20^\circ\text{C}$

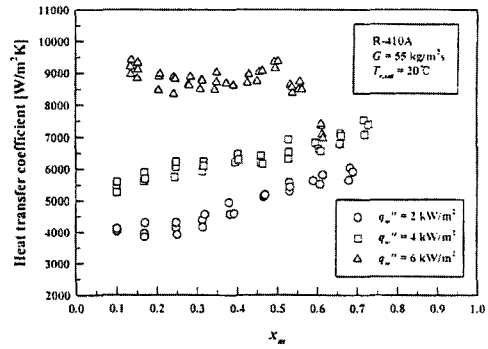


Fig. 5 Variation of evaporation heat transfer coefficient with mean vapor quality for various heat fluxes at  $G=55\text{kg/m}^2\text{s}$  and  $T_{r,sat} = 20^\circ\text{C}$

The effect of the average heat flux on the evaporation heat transfer is shown Fig. 5 by presenting the heat transfer data for heat fluxes ranging from 2.0 to 6.0  $\text{kW/m}^2$  at  $G=55\text{kg/m}^2\text{s}$  and  $T_{r,sat}=20^\circ\text{C}$ . It is well known that the evaporation rate would be proportional to the heat flux. The results indicate that at a given vapor quality the heat transfer coefficient is higher for a higher heat flux except at  $x_m > 0.5$  with 6.0  $\text{kW/m}^2$ . It is important to note that at the high vapor quality with  $x_m > 0.6$  the heat transfer coefficient for  $q_w''=4\text{ kW/m}^2$  is much higher than that for the higher wall heat flux  $q_w''=6\text{ kW/m}^2$ . This is attributed to the fact that at a high vapor quality the wall may become partially dry when the wall heat flux is high enough. Obviously, the evaporation heat transfer deteriorated on the partially dry wall. For the case at the low heat flux the wall remains wet even at a high vapor quality. Moreover, at this vapor quality the vapor velocity is high and the convective evaporation is rather strong. Thus  $h_r$  increases with  $x_m$  for the entire range of the vapor quality for  $q_w''=4$

$\text{kW/m}^2$ .

The effects of the refrigerant saturation temperature on the evaporation heat transfer coefficient is illustrated in Fig. 6 by presenting the data for two typical cases at  $G=55 \text{ kg/m}^2\text{s}$  and  $q_w''=6.0 \text{ kW/m}^2$  at different mean vapor qualities for  $T_{r,\text{sat}}$  ranging from 15 to  $20^\circ\text{C}$ . The results suggest that at a given saturation temperature the evaporation heat transfer coefficient rises significantly with the mean vapor quality. While at a fixed  $x_m$ , the evaporation heat transfer coefficient is poorer at a higher  $T_{r,\text{sat}}$  in the total quality region. Specifically, the mean heat transfer coefficient at  $15^\circ\text{C}$  is about 20% bigger than that at  $20^\circ\text{C}$ .

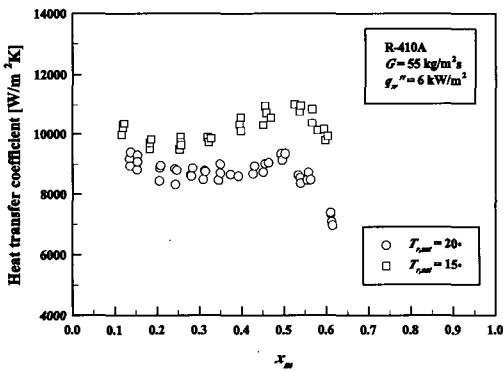


Fig. 6 Variation of evaporation heat transfer coefficient with mean vapor quality for various saturation temperatures at  $G = 55 \text{ kg/m}^2\text{s}$  and  $q_w'' = 6 \text{ kW/m}^2$

Fig. 6 indicates that there are two distinct heat transfer regions in flow boiling of refrigerant. The first is a partial boiling region occurring at low qualities in which heat transfer coefficients are a strong function of heat flux. Both the forced convective evaporation and nucleate boiling mechanisms were found to be responsible for the heat transfer in this

region. The rapid suppression of the latter even leads to a temporary reduction of the heat transfer coefficients with increasing quality as shown in Fig. 6, which was observed also with smooth tube. The second is a convective evaporation region beyond the transition quality where heat transfer coefficients are independent of heat flux. The present results advocate a conventional concept of the suppression of nucleate boiling with increasing quality. As quality is increased, the effective wall superheat decreases due to a thinner liquid film (less thermal resistance) and an enhanced convection caused by high vapor velocity. Thus, the number of active nucleation sites decreases till a transition quality is reached. Beyond the transition quality, the effective wall superheat is below the value required for bubble nucleation on the wall.

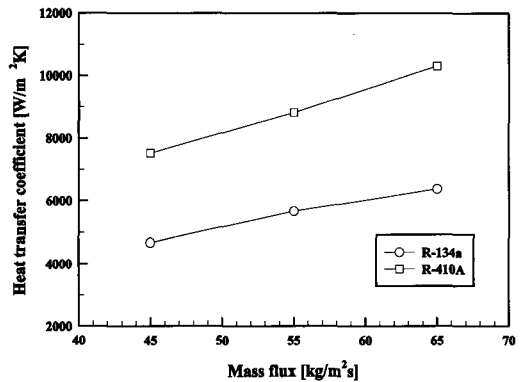


Fig. 7 Evaporation heat transfer coefficient with refrigerant at  $q_w'' = 6 \text{ kW/m}^2$  and  $T_{r,\text{sat}} = 20^\circ\text{C}$

It is necessary to compare the present data for the R-410A evaporation heat transfer coefficient to that for another refrigerant. Due to the limited availability of the data for shell and plate heat



exchanger with the same ranges of the parameters covered in the present study. The comparison is only possible for our cases. This is illustrated in Fig. 7, the comparison clearly shows that R-410A evaporation heat transfer coefficient is about 60% in average higher than that for R-134a<sup>(10)</sup>.

### 4.3 Correlating equation

To facilitate the use of S&PHE as evaporators, correlating equation for the dimensionless evaporation heat transfer coefficient based on the present data is provided. This is modified form of Yan et al. correlation<sup>(11)</sup>.

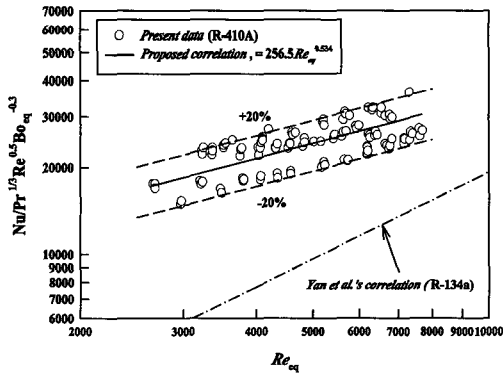


**Fig. 8 Comparison of the proposed correlation for the evaporation heat transfer coefficient with the present data**

$$N/Pr^{1/3} Re^{0.5} Bo_{eq} = 256.5 Re_{eq}^{0.534} \quad (15)$$

Where  $Re_{eq}$  and  $Bo_{eq}$  are, respectively, the equivalent Reynolds and Boiling numbers in which an equivalent mass flux is used in their definitions first proposed by Akers et al.<sup>(12)</sup>.

$$Re_{eq} = \frac{G_{eq} D_h}{\mu_l} \quad \text{and} \quad (16)$$

where

$$G_{eq} = G \left( 1 - x_m + x_m \left( \frac{\rho_l}{\rho_v} \right)^{1/2} \right) \quad (17)$$

Fig. 8 illustrates the comparison of the proposed correlation to the present data. It is found that the average deviation is about  $\pm 20\%$  between the correlation and the data.

## 5. Conclusion

An experimental investigation has been conducted in the present study to measure the evaporation heat transfer coefficient of R-410A in a shell and plate heat exchanger. The effects of the mass flux of R-410A, average imposed heat flux, saturation temperature and vapor quality of R-410A on the measured data were examined in detail.

The results showed that the evaporation heat transfer coefficients increased with the refrigerant mass flux. Similar to the mass flux effects, the heat flux had significant effects on the heat transfer at high quality. The increase in the saturation temperature resulted in a lower heat transfer coefficient in the total vapor quality regime.

The empirical correlation was provided for the measured heat transfer coefficients in terms of the Nusselt number.

## Acknowledgement

This work has been supported by Regional Research Center for Advanced Environmentally Friendly Energy Systems of Pukyong National University.

## References

- [1] Kerner, J., Sjogren, S. and Svensson, L., "Where Plate Exchangers Offer Advantages Over Shell-and-Tube," *Power*, Vol. 131, pp. 53-58, 1987.
- [2] Williams, B., "Heat Transfer Savings on a Plate," *Heating and Air Conditioning Journal*. Apt., pp. 29-31, 1996.
- [3] K-B Lee, M-G Seo, J-H Park and Y-S Kim, "An Experimental Study on Pressure Drop Characteristics in Plate and Shell Heat Exchanger," *Journal of the Korean Society of Marine Engineers*, Vol. 25, pp. 1220-1227, 2001.
- [4] K-B Lee, J-H Park, M-G Seo, H-W Lee and Y-S Kim, "Experimental Study on R-134a Condensation Heat Transfer Characteristics in Plate and Shell Heat Exchanger," *Journal of the Korean Society of Marine Engineers*, Vol. 27, pp. 108-115, 2003.
- [5] Shah, R. K. and Wanniarachchi, A. S., "Plate Heat Exchanger Design Theory in Industry Heat Exchanger," in J. M. Buchlin (Ed.), *Lecture Series*, No. 1991-04, Von Karman Institute for Fluid Dynamics, Belgium, 1992.
- [6] Farrell, P., Wert, K. and Webb, R., "Heat Transfer and Friction Characteristics of Turbulent Radiator Tubes," *SAE Technical Paper series*, No. 910197, 1991.
- [7] Sieder, E. N. and Tate, G. E., "Heat Transfer and Pressure Drop of Liquids in Tubes," *Int. Eng. Chem.*, Vol. 28, pp. 1429-1435, 1936.
- [8] Wilson, E. E., "A Basis for Rational Design of Heat Transfer Apparatus," *Trans. ASME*, Vol. 37, pp. 47-70, 1915.
- [9] Kline, S. J. and McClintock, F. A., "Describing Uncertainties in Single-Sample Experiments," *Mechanical Engineering*, Vol. 75, No. 1, pp. 3-12, 1953.
- [10] Seo, M. G., "Heat Transfer and Pressure Drop Characteristics of the Plate and Shell Heat Exchanger," *Univ. of Pukyong, Ph.D. Thesis*, 2002.
- [11] Yan, Y., Lio, H. and Lin, T., "Evaporation Heat Transfer and Pressure Drop of Refrigerant R-134a in a Plate Heat Exchanger," *J. Heat Transfer*, Vol. 121, pp. 118-127, 1999.
- [12] Akers, W. W., Dean, H. A. and Crosser, O., "Condensation Heat Transfer Within Horizontal Tubes," *Chem. Eng. Prog.* 54, pp. 89-90, 1958.

## 저 자 소 개



박재홍 (朴載弘)

August, 1999, B.S., Refrigeration and Air-Conditioning Eng., Pukyong National University, August, 2001, M.D., Refrigeration and Air-Conditioning Eng., Pukyong National University, (Present) Ph.D. Candidate Refrigeration and Air-Conditioning Eng., Pukyong National University.



**김인관 (金仁官)**

February. 1994, B.S., Die&Mold Eng., Pukyong National University, August. 1996, M.D., Die&Mold Eng., Pukyong National University, Ph.D., February. 2004, Refrigeration and Air-Conditioning Eng., Pukyong National University, (Present) Regional Research Center for Advanced Environmentally Friendly Energy Systems, Pukyong National University Professor (CAEFES)



**김영수 (金永守)**

February. 1979, B.S., Mechanical Eng., Pusan National University, February. 1981, M.S., Mechanical Eng., Seoul National University, May. 1994, Ph.D., Mechanical Eng., Concordia University in Canada, (Present) School of Mechanical Eng., Pukyong National University Professor